Journal of the Civil Engineering Forum, September 2025, 11(3):341-352
DOI 10.22146/jcef.18303
Available Online at https://jurnal.ugm.ac.id/v3/jcef/issue/archive

Compressive and Flexural Properties of the Kevlar Fiber as a Textile-Reinforced Concrete for Lightweight Construction Applications

Hendra[1,2*], Syahla Andini Putri[3], Muhammad Arief Herdianto[4]
[1]Department of Applied Sciences in Textile Engineering and Apparel Technology, Politeknik STTT Bandung, Bandung, INDONESIA
[2]Department of Materials Innovation, University of Tsukuba, Tsukuba, Ibaraki, JAPAN
[3]Department of Textile Chemistry, Politeknik STTT Bandung, Bandung, INDONESIA
[4]Department of Textile Engineering, Politeknik STTT Bandung, Bandung, INDONESIA
*Corresponding author: hendramahesa@yahoo.com

SUBMITTED 12 December 2024 **REVISED** 2 July 2025 **ACCEPTED** 3 July 2025

ABSTRACT Textile-reinforced concrete (TRC) offers a sustainable alternative to conventional steel-reinforced concrete by incorporating textile elements, thereby reducing carbon emissions and enhancing design flexibility. This study examines the use of Kevlar fiber reinforcement in improving the mechanical performance of concrete, with particular attention to compressive and flexural properties. Three Kevlar reinforcement configurations were evaluated: 3-dimensional (3D) rebar, 3D hollow woven fabric, and solid 3D woven fabric, alongside a control sample of unreinforced concrete. Compression tests were conducted in accordance with SNI 03-1974-1990, which is broadly equivalent to ASTM C39 in terms of loading procedure and specimen dimensions. Results showed that the 3D rebar configuration achieved the highest compressive strength of 14.31 MPa, marginally exceeding that of the unreinforced control at 13.28 MPa. Although the gains in compressive strength were modest, the flexural performance exhibited substantial improvement. Flexural tests, following ASTM C78 standards, revealed that the solid 3D woven fabric configuration achieved a flexural strength of 12.17 MPa, whereas that of unreinforced sample was 3.65 MPa. These results indicate that Kevlar-reinforced TRC can be particularly advantageous for applications where superior flexural capacity is required, even if compressive strength remains at a moderate level. Potential uses include non-structural or secondary lightweight elements, such as canopies, facade panels, and other architectural components where weight reduction, crack resistance, and design adaptability are desirable. The findings also highlight the influence of reinforcement configuration, with the solid 3D woven fabric providing the most significant flexural benefits. This research contributes to the growing body of evidence supporting the viability of synthetic fiber reinforcement, such as Kevlar, in sustainable concrete design and construction.

KEYWORDS 3D rebar configuration, 3D hollow configuration, 3D solid configuration, Textile Reinforced Concrete, and Kevlar fiber

1 INTRODUCTION

Textile materials such as fibers, yarns, or fabrics have gained increasing attention for applications beyond traditional garments. Their versatility has enabled their use in the medical and healthcare sectors (Cheung and Li, 2019), aerospace (Abidin et al., 2019), marine industries (Aravind et al., 2022; Sankaran et al., 2016), smart and wearable textiles (Dalkılıç et al., 2024; Najafi et al., 2017; Coskun and Oner, 2022), food packaging (Carneiro da Silva et al., 2023), and construction (Friese et al., 2022; Hahn et al., 2021; Krimi et al., 2016; Koeckritz et al., 2010).

In the construction sector, textile materials have been increasingly used as reinforcement in concrete, commonly referred to as textile-reinforced concrete (TRC). Compared to conventional steel reinforcement, textile reinforcement offers several advantages, including resistance to corrosion, chemical degradation, and UV exposure (Lin et al., 2022; Seyam et al., 2015; Yan and Chouw, 2013). Steel reinforcement, while effective, remains vulnerable to corrosion in aggressive environments such as coastal zones, which often requires thicker concrete cover and results in higher cement usage. By contrast, non-corrosive textile reinforcement enables thinner concrete sections, reducing both material usage and environmental impact (Laiblová et al., 2019). Although the production of textile reinforcements generates CO_2 emissions, the reduction in cement content, the largest contributor to concrete's carbon footprint, can lead to net environmental benefits (Li and Xu, 2011). For instance, in a German cyclist bridge project, textile reinforcement reduced cement usage by 60% and emissions by 26% compared to steel-reinforced alternatives.

Numerous studies have assessed the mechanical performance of TRC. For instance, Gopinath et al. (2015) showed that basalt TRC blocks absorbed 25 – 30% more energy under compression than plain concrete. Islam et al. (2023) reported that carbon textiles exhibited the highest flexural strength (11.2 MPa) in cement panels, followed by glass (7.8 MPa) and GI fibers (6.1 MPa).

These findings affirm the role of fiber type in defining TRC mechanical behavior.

Beyond material selection, structural geometry significantly influences TRC performance. Verma and Majumdar (2024) examined three types of 3D-knitted textiles with spacer thread angles of 65°, 55°, and 47°, and found that a smaller thread angle of 47° led to higher compressive strength. This result highlights the role of geometrical optimization in improving mechanical interlocking and load distribution within textile-reinforced composites.

Reinforcement configurations are generally categorized as 1D (linear fibers), 2D (woven, knitted, or spacer fabrics), or 3D (braided, stitched, or embroidered textiles) (Wu et al., 2023). While 1D and 2D configurations primarily enhance in-plane strength, they offer limited resistance to out-of-plane stresses and are susceptible to delamination (Perera et al., 2021). In contrast, 3D textile architectures provide through-thickness reinforcement, enabling better load transfer and damage tolerance (Hu et al., 2020). Although some studies have investigated 3D textile reinforcement in TRC, this area remains relatively underexplored compared to 1D and 2D configurations. Wu et al. (2023) highlighted the potential of 3D textile-reinforced concrete, specifically its superior out-of-plane load resistance, delamination suppression, and improved damage tolerance compared to 2D systems. Nevertheless, the same study also emphasized that further investigation is needed to develop quantitative design models, evaluate long-term durability under environmental exposure, and assess manufacturing scalability for real-world structural applications (Wu et al., 2023).

Kevlar, a high-performance aramid fiber, possesses an exceptional strength-to-weight ratio, energy absorption, and chemical stability, making it an attractive candidate for TRC (Ursache et al., 2024). Unlike carbon or glass fibers, Kevlar is flexible and crack-resistant, and unlike steel, it does not corrode (Shafei et al., 2021). Despite its favorable properties, Kevlar is underutilized in TRC research. Early studies focused on short or continuous Kevlar fibers in cement (Walton and Majumdar, 1978), with limited exploration of Kevlar-based textile reinforcements.

Reinforcement configurations in most structural elements, such as beams, columns, and shear walls, are inherently three-dimensional (3D) to accommodate complex loading conditions, including axial forces, shear, bending moments, and torsion. Traditional reinforcement using steel bars is intentionally arranged in 3D space to ensure effective load transfer and structural stability. However, most studies on TRC focused on 1D or 2D textile geometries, which may not may not fully reflect actual structural conditions. Therefore, this study aims to develop three novel 3D Kevlar textile reinforcement configurations: (1) 3D-rebar, (2) hollow 3D woven fabrics, and (3) solid 3D woven fabrics, and to investigate their effects on the mechanical performance and damage tolerance of textile-reinforced concrete. These reinforcements were manually constructed and integrated into TRC specimens, as schematically illustrated in Figure 1 (a – c) and visually depicted inside the mold in Figure 1 (d – f). To the best of our knowledge, the mechanical behavior and structural benefits of such 3D Kevlar reinforcement forms in TRC have not been systematically studied. This research aims to fill that gap by evaluating their effectiveness in enhancing mechanical interlocking, anchorage, and overall load-bearing performance.

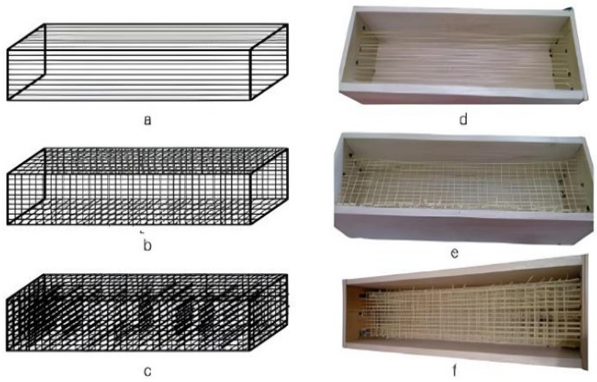

Figure 1 (a) Schematic illustration of the 3-dimensional rebar, (b) 3-dimensional hollow woven fabric, and (c) solid 3-dimensional woven fabric. (d) Photograph of the 3D-manufacturing of the 3-dimensional rebar, (e) 3-dimensional hollow woven fabric, and (f) solid 3-dimensional woven fabric.

The mechanical behavior of the resulting composites was evaluated through compressive and flexural testing and compared to control samples of plain concrete. This study provides insight into how textile geometry and material properties interact to improve mechanical performance, thereby supporting the development of lighter, more durable, and environmentally sustainable concrete systems.

2 METHODS

It is important to note that the number of samples used for each variable in this study was limited to a single specimen per treatment due to constraints in material availability and access to specialized testing equipment. Nevertheless, all experiments were conducted under strictly controlled and consistent conditions to ensure the reliability of the comparative analysis.

2.1 Materials

The Kevlar fiber used in this study was in the form of yarns with a tenacity of 18 g/denier (≈1.58 MPa) and a linear density of approximately 3200 denier. The

elongation at break was about 3.2%. The yarns were procured from PT. Kusumah Mandiri Jakarta and used without further treatment.

Ordinary Portland Cement (OPC), conforming to ASTM C150 Type I, was used as the matrix material due to its widespread availability and suitability for general structural applications. The cement was obtained from a local supplier and stored in a dry environment to prevent moisture absorption. The specific gravity of the cement, determined using the Le Chatelier flask method according to ASTM C188, was found to be 3.15. A water-to-cement ratio of 0.45 was selected to ensure optimal workability and matrix density, aligning with established practices in TRC fabrication (Brameshuber, 2006). Natural river sand passing through a 4.75 mm sieve was used as fine aggregate. This particle size conforms to standard classifications for fine aggregates and ensures good workability, uniform dispersion, and effective bonding with the Kevlar textile reinforcements (Wang et al., 2024). The finer sand size also minimizes voids and reduces the likelihood of damage to the textile during casting.

2.2 Fabrication of the 3-Dimensional Kevlar Fiber Configuration

The sample preparation process for the three 3D configurations, namely rebar, hollow woven fabric, and solid woven fabric, was schematically illustrated in Figure 2.

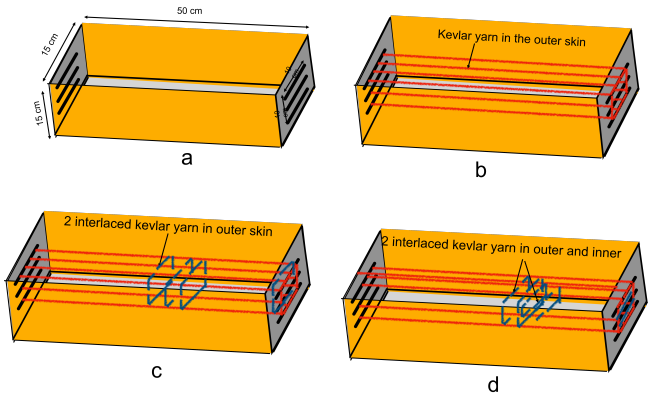

Figure 2 Schematic representation of the fabrication steps for (a) mold samples, (b) 3D rebar configuration, (c) 3D hollow woven fabric, and (d) 3D solid woven fabric.

The fabrication process began with mold preparation. A rectangular wooden mold was constructed using four wooden boards. Two of the boards (15 cm × 15 cm) were drilled with holes at a density of 4 holes/cm^2, confined to a central 10 cm × 10 cm region, while the outer areas were left intact. The other two boards (50 cm × 15 cm) were not drilled. These boards were assembled into a mold with internal dimensions of 15 cm (width) × 50 cm (length), used as the casting form for the concrete specimens. A schematic of the mold setup is presented in Figure 2 (a).

The rebar-like configuration was produced by threading Kevlar yarn through the drilled holes on the shorter mold walls to create a unidirectional network across the mold's width. The yarns were laid in a back-and-forth pattern in a parallel arrangement, forming a surface-layer reinforcement on both ends while leaving the central core region unreinforced.

During the fabrication of the 3D Kevlar textile configurations, a controlled tension was applied to the yarns to maintain alignment, prevent sagging, and ensure dimensional stability of the reinforcement. This approach helped achieve uniform geometry and promoted effective interaction between the textile and cementitious matrix during casting. A schematic illustration of this configuration is shown in Figure 2 (b).

The 3D hollow woven fabric configuration was formed by manually weaving two sets of Kevlar yarns, warp and weft, in perpendicular directions to form a hollow, fabric-like mesh. The interlacing was applied only around the perimeter of the mold cavity, creating a reinforced outer shell while the inner core remained free of reinforcement. The yarns were woven inside the mold with careful alignment and tension control. Tension was maintained by carefully laying the yarns by hand to keep them straight.

This hollow 3D woven structure provides bidirectional reinforcement on the outer layer while reducing overall material weight. A schematic illustration of the fabrication process is shown in Figure 2 (c).

The solid woven configuration extends the hollow woven concept by continuing the yarn interlacing throughout the entire volume of the mold. Kevlar yarns were manually woven layer by layer, from the bottom to the top, in both warp and weft directions. This produced a densely packed, fully integrated 3D textile reinforcement. Unlike the hollow version, the solid configuration provides uniform reinforcement across all cross-sectional planes, enhancing both longitudinal and transverse mechanical performance. The final configuration offers uniform strength distribution, making it suitable for demanding structural applications (Hu et al., 2020). A schematic illustration of this configuration is shown in Figure 2 (d).

2.3 Fabrication and Characterization of the Textile Reinforced Concrete

The standard mix ratio for the control concrete (without fibers) was selected based on established practices for general-purpose structural concrete. A cement content of 400 kg/m^3 and a water-to-cement ratio of 0.45

were used to ensure a balance between workability and strength development, typically targeting compressive strengths of 30 – 40 MPa. A fine-to-coarse aggregate ratio of 1:2 was used to achieve good aggregate gradation and minimize segregation. This mix serves as a baseline for evaluating the effect of Kevlar yarn reinforcement in the modified samples. The mixed matrix was then poured into molds containing Kevlar fibers in different configurations, ensuring that the molds were fully filled with the matrix, and cured for 10 days, as shown in Figure 3.

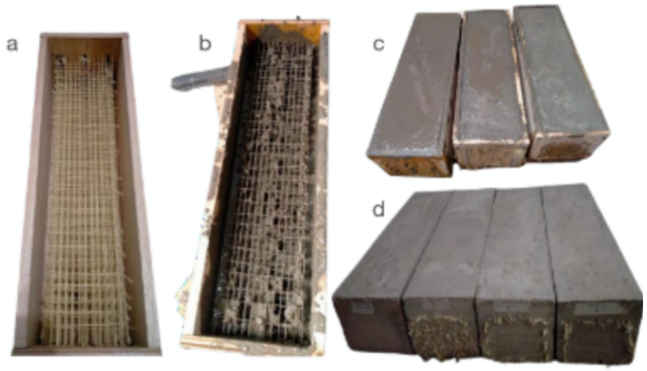

Figure 3 Manufacturing process of Kevlar-reinforced concrete: (a) Kevlar configuration placed within the mold, (b) pouring of the cement matrix into the mold, (c) mold fully filled with the cement matrix, and (d) cured Kevlar-reinforced concrete.

The fiber-to-concrete ratios for the 3D rebar, 3D hollow woven fabric, and 3D solid woven fabric configurations were 0.03%, 0.05%, and 0.17%, respectively. These differences reflect the inherent structural geometry and fiber requirements of each configuration. The ratios were calculated based on the total weight of Kevlar yarn used relative to the weight of the final concrete. Although this approach introduces variation in fiber content, the fiber amounts were intentionally not normalized to preserve the structural integrity and practical implementation of each reinforcement type. This decision was made to better simulate the realistic application of lightweight construction, such as a canopy, and was considered when interpreting mechanical performance results.

The concrete samples were characterized through compressive strength testing and 3-point bending tests. The 3-point bending test was employed to assess the flexural performance and crack resistance of the fiber-reinforced concrete. This method is particularly suitable for capturing the influence of fiber configuration on tensile stress distribution, ductility, and post-cracking behavior under bending loads. For the compressive test, the samples were cut into cubes measuring 15 cm × 15 cm × 15 cm. The compressive strength test was conducted using a universal testing machine at the Materials Laboratory, Institut Teknologi Bandung, following the Indonesian standard SNI 03-1974-1990, which specifies procedures for testing concrete compressive strength. This standard is broadly equivalent to international standards such as ASTM C39 in terms of loading procedure and specimen dimensions. The samples were subjected to loading at a constant rate of 4 kg/cm² per second until failure. The maximum load applied before failure was recorded as the fracture load. The bending test was performed using a Tensolab testing machine with a 3-point bending test. Samples measuring approximately 150 mm × 150 mm in cross-section and 500 mm in length were placed on the testing machine with a span length of 400 mm. The compressive strength was calculated using Equation 1:

$$\sigma = \frac{F}{A} \tag{1}$$

where σ is the compressive stress, F is the load (force) applied to the sample (kN), and A is the cross-sectional area of the sample (mm^2), measured before the experiment.

The compressive modulus of the tested sample was calculated using Equation 2:

$$E_c = \frac{\sigma}{\varepsilon} \tag{2}$$

where E_c is the compressive modulus, σ is the compressive strength (MPa), and ε is the compressive strain (%).

The flexural strength of the sample was calculated using Equation 3:

$$f_s = \frac{3PL}{2bd^2} \tag{3}$$

where f_s is the flexural strength (MPa), P is the maximum applied load at fracture (kN), L is the span length between supports (cm), b is width of the concrete sample (mm), and d is depth (height) of the concrete sample (mm). The flexural modulus of the sample was calculated using Equation 4:

$$E_f = \frac{PL^3}{4\delta bd^2} \tag{4}$$

where E_f is the flexural modulus (MPa), P is the applied load at the center of the beam (kN), L is the span length between the two supports (cm), δ is the deflection at the center of the beam measured using Linear Variable Differential Transformer (LVDT) (mm), b is the width of the concrete sample (mm), and d is the depth (height) of the concrete sample (mm).

3 RESULTS AND DISCUSSION

The study focuses on evaluating the mechanical performance of newly developed Kevlar reinforcement configurations, which to the best of the author's knowledge, have not been previously reported in the literature.

Therefore, the data obtained provide original and valuable insights into the effects of varying Kevlar architectures on the mechanical behavior of cementitious composites. While additional testing with larger sample sizes is encouraged to further substantiate these findings, the current results make a meaningful contribution to the development of civil engineering materials and provide a solid foundation for future research in this field.

3.1 The Effect of Kevlar Configuration on the Compressive Properties of the Kevlar Reinforcement Concrete

According to the load – displacement curves obtained from the compressive test, as depicted in Figure 4, the 3D rebar configuration (Figure 4(a)) exhibited the highest load-bearing capacity, achieving a maximum load of approximately 315 kN at a relatively low actuator displacement of 2.8 mm, indicating both high strength and stiffness. In comparison, the 3D hollow configuration (Figure 4(b)) reached a peak load of about 287 kN with an actuator displacement of approximately 3.3 mm, suggesting lower strength and slightly greater deformation compared to the rebar configuration. The 3D solid configuration (Figure 4(c)) sustained a peak load of about 290 kN with a displacement of 3.2 mm, indicating a balance between load capacity and deformation. Lastly, the blank concrete sample (Figure 4(d)), without any reinforcement, achieved a maximum load of about 300 kN with an actuator displacement of 3.75 mm, indicating lower stiffness and higher ductility compared to the reinforced specimens. These results suggest that reinforcement, particularly with the 3D rebar configuration, significantly enhances both the strength and stiffness of the composite material. Table 1 and Figure 4 depicted the result of the compressive strength test.

The compressive strength of textile-reinforced concrete samples incorporating Kevlar yarn in 3D rebar, 3D hollow woven fabric, and solid 3D woven fabric configurations is presented in Table 1. In addition, a bar chart comparing the compressive strength of these samples, along with concrete without Kevlar fibers (blank concrete), is shown in Figure 5.

As shown in Table 1 and Figure 5, the blank concrete exhibited a compressive strength of 13.28 MPa, while the concrete samples reinforced with 3D rebar, 3D hollow woven fabric, and 3D solid woven fabric configurations achieved compressive strengths of 14.31 MPa, 12.3 MPa, and 13.07 MPa, respectively. These results indicate that there is no clear linear correlation between compressive strength and the Kevlar configuration or fiber content.

Table 1. Compressive strength of the Kevlar Reinforced Concrete

No	Configurations	CS (MPa)
1	Blank concrete	13.28
2	3D rebar	14.31
3	3D hollow woven fabric	12.30
4	Solid 3D woven fabric	13.07

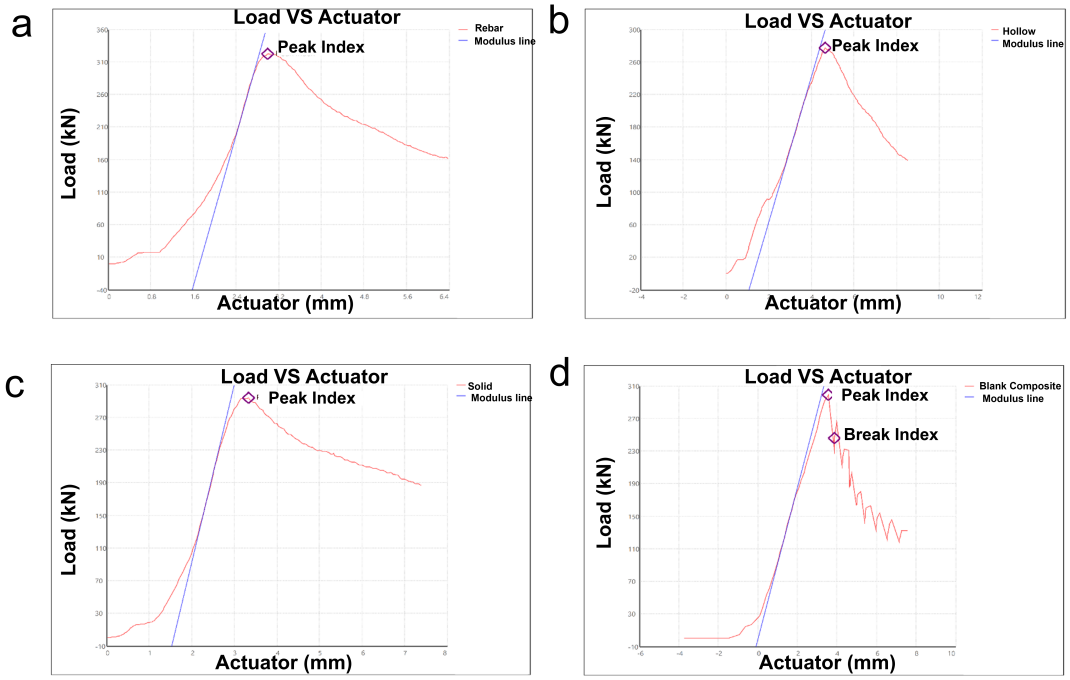

Figure 4 Load-displacement curve obtained from the compressive test, illustrating the relationship between the applied load (kN) and actuator displacement (mm). The curve is divided into four sections: (a) rebar configuration, (b) 3D hollow configuration, (c) 3D solid configuration, and (d) blank concrete.

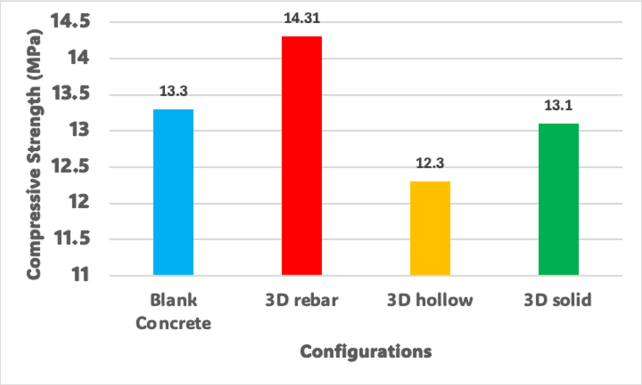

Figure 5 Compressive strength of the Kevlar-reinforced concrete.

The blank concrete showed a higher compressive strength than the samples reinforced with 3D hollow woven fabric and solid 3D woven fabric, which show reductions in compressive strength of approximately 8% and 1.6%, respectively. However, the 3D rebar configuration demonstrated the highest compressive strength among other reinforced samples.

This behavior can be attributed to the fact that woven fabric reinforcement is often more related to improving ductility, toughness, and crack resistance, rather than directly increasing compressive strength (Bartulović et al., 2022). The fibers facilitate more uniform stress distribution within the material, thereby reducing crack initiation and propagation under load (Neves and Felicíssimo, 2020). However, they do not necessarily contribute to the ultimate compressive strength. Instead, the woven fabric enhances energy absorption capacity and improves post-cracking behavior (El-Feky et al., 2024). This finding is supported by the visual evidence in Figure 6, which shows that concrete samples with higher Kevlar fiber content exhibited less severe cracking and more distributed failure patterns compared to those with lower fiber content. These observations confirm that woven reinforcement plays a crucial role in crack mitigation and energy dissipation, even though it may not enhance the compressive strength.

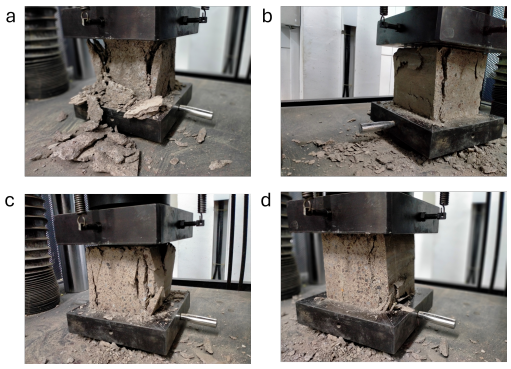

Figure 6 Cracking patterns of the samples after the compressive test: (a) blank concrete, (b) concrete with 3D rebar, (c) concrete with 3D hollow woven fabric, and (d) concrete with 3D solid woven fabric.

3.2 The Effect of Kevlar Configuration on the Compressive Modulus of Kevlar Reinforcement Concrete

Table 2 and Figure 7 present the compressive modulus for the Kevlar-reinforced concrete samples, while Figure 6 illustrates the cracking patterns observed in the samples during the compressive test.

The fiber content in the 3D rebar, 3D hollow woven fabric, and solid 3D woven fabric configurations was 0.03%, 0.05%, and 0.17%, respectively. It is evident that the compressive modulus decreases with increasing fiber content. This trend can be explained theoretically and is supported by previous studies (Mahadik and Hallett, 2022; Zhang et al., 2010), which reported that increasing fiber content in dense 3D woven configurations may lead to higher porosity due to packing constraints, thereby reducing overall density and stiffness. Since porous materials are generally less stiff and more susceptible to deformation under load, this results in a lower compressive modulus (Ghasemi et al., 2024).

Moreover, Kevlar fibers are hydrophobic, which limits their ability to form strong interfacial bonds with the cement matrix (Bentur and Mindess, 1990). As the fiber content increases, this poor bonding may result in ineffective load transfer, thereby reducing the overall resistance to compressive deformation (Sarwar et al., 2022).

Additionally, higher fiber content can lead to uneven distribution and misalignment, especially in complex configurations such as solid 3D woven fabric. Improper fiber alignment may compromise the reinforcing effectiveness, leading to irregular stress distribution and reduced stiffness.

Table 2. Compressive modulus of the Kevlar reinforced concrete

No	Configurations	CM (GPa)
1	Blank concrete	33.7
2	3D rebar	36.4
3	3D hollow woven fabric	19.8
4	Solid 3D woven fabric	29.6

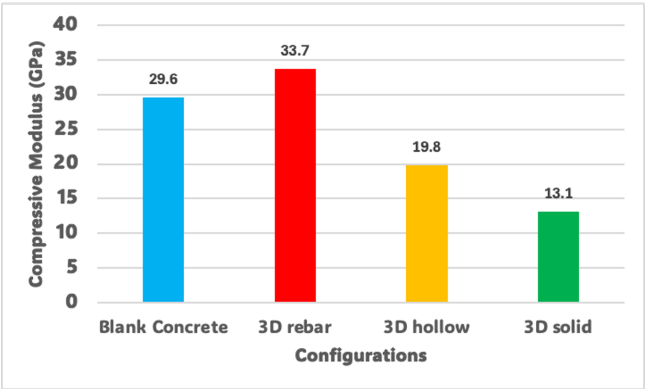

Figure 7 Compressive modulus of the Kevlar-reinforced concrete.

3.3 The Effect of Kevlar Configuration on the Flexural Strength of the Kevlar Reinforcement Concrete.

The results of the three-point bending test, shown as load-displacement curves in Figure 8, highlight the distinct flexural behaviors of the different reinforcement configurations. The rebar-reinforced concrete showed moderate performance, reaching a maximum load of 22.5 kN at an actuator displacement of 4.5 mm. Although effective in compression, the 3D rebar reinforcement provided limited flexural resistance in this setup, indicating suboptimal performance in bending. The 3D hollow woven Kevlar configuration showed improved performance, achieving a maximum load of 32 kN at approximately 4.5 mm displacement. This result suggests a more favorable balance between strength and stiffness, with greater energy absorption compared to the 3D rebar configuration sample. Among all tested samples, the 3D solid woven Kevlar configuration demonstrated the highest flexural strength, reaching a maximum load of 62 kN at 7 mm displacement. The extended load-displacement response reflects superior load-bearing capacity and ductility under bending. In contrast, the blank concrete showed the weakest performance, failing at a maximum load of 17 kN with a displacement of only 1.5 mm. This brittle response highlights the critical role of reinforcement in enhancing flexural behavior. Overall, the results indicate that the 3D solid woven Kevlar configuration is the most effective configuration for improving flexural strength and ductility, while the rebar and blank concrete provide limited resistance under bending.

From Table 3, it can be observed that the weight fraction of Kevlar yarn and its configuration strongly correlate with flexural strength. The flexural strength increased progressively from 3.65 MPa for the blank concrete (0% fiber content), followed by 4.53 MPa for the 3D rebar configuration (0.03% fiber content), 6.72 MPa for the 3D hollow woven fabric (0.05% fiber content), and up to 12.17 MPa for the solid 3D woven fabric (0.17% fiber content). This correlation is clearly illustrated in Figure 9. These results suggest that fiber content plays a direct role in enhancing crack resistance. Concrete is particularly prone to micro-cracking under tensile stress during bending, and the data indicate that increasing fiber content leads to higher flexural strength.

Table 3. Flexural strength of the Kevlar Reinforced Concrete

No	Configurations	FS (MPa)
1	Blank concrete	3.65
2	3D rebar	4.57
3	3D hollow woven fabric	6.72
4	Solid 3D woven fabric	12.17

The alignment and uniform distribution of fibers in the solid 3D woven fabric enhance its performance by improving tensile stress resistance and flexural strength. This configuration facilitates more efficient stress transfer through increased fiber – matrix contact area, which in general can contribute to stronger interfacial bonding as reported in prior studies (Lyu et al., 2022; Nguyen et al., 2013). However, it should be noted that these studies address the effect of contact area

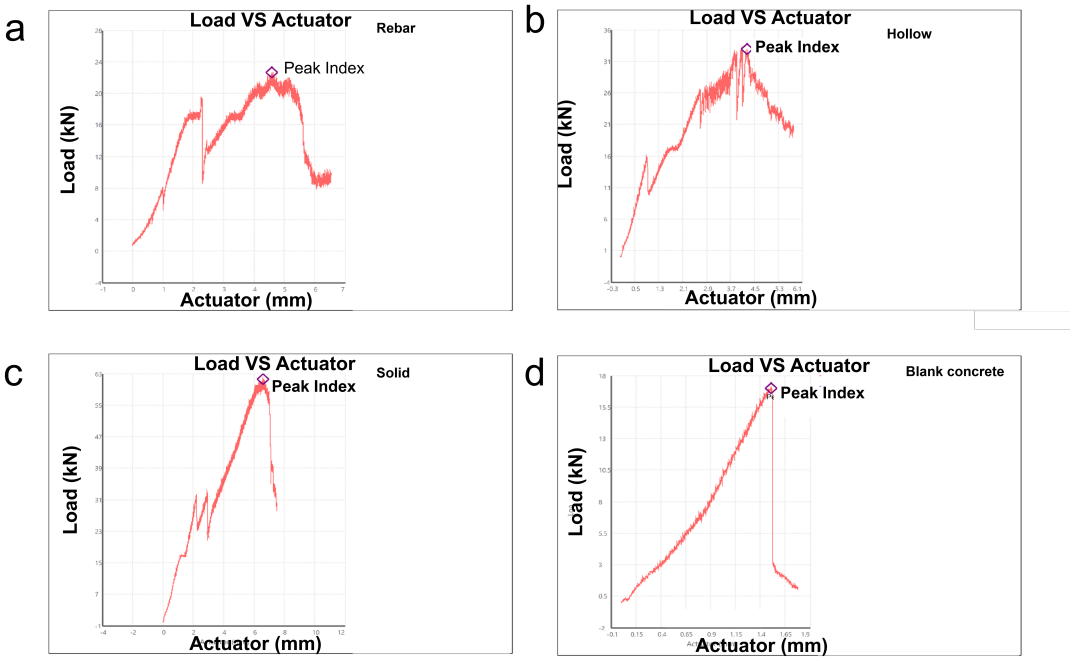

Figure 8 Load – displacement curve obtained from the flexural test, showing the relationship between applied load (kN) and actuator displacement (mm). a) rebar configuration, b). 3-d hollow configuration, c). solid 3-d configuration, and d). blank composite.

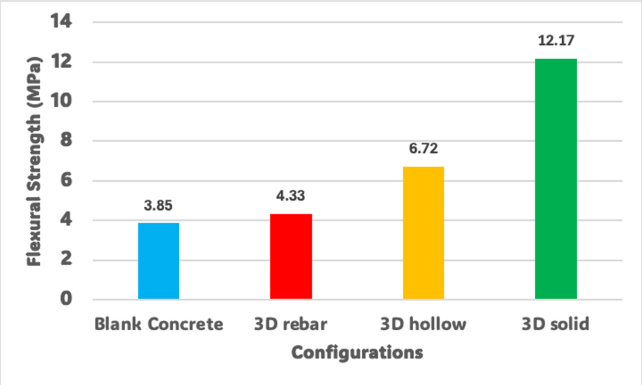

Figure 9 Graphical image of the flexural strength of the Kevlar reinforced concrete.

on interfacial bonding without specific consideration of the hydrophobic nature of Kevlar fibers. The presence of Kevlar fibers in concrete promotes a more uniform strength distribution by bridging microcracks and redistributing stress, thereby delaying failure and minimizing localized weakness (Nelson et al., 2002). As shown in Figure 10, cracks in Kevlar-reinforced concrete tend to initiate predominantly near the center of the specimen, while cracking in blank concrete appears more randomly distributed. Although this observation does not directly quantify stress distribution on the beam samples, the cracking pattern suggests a more controlled failure mode in the presence of Kevlar reinforcement.

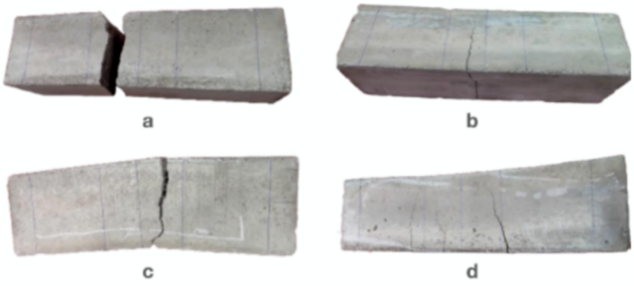

Figure 10 The cracking point area of the samples after the three-point bending test: (a) blank concrete, (b) 3D rebar, (c) 3D hollow woven fabric, and (d) 3D solid woven fabric.

3.4 The Effect of Kevlar Configuration on the Flexural Modulus of the Kevlar Reinforcement Concrete

The flexural modulus showed a nonlinear trend across different Kevlar configurations and fiber contents, as illustrated in Figure 11 and summarized in Table 4. The blank concrete exhibited the highest flexural modulus, indicating greater stiffness than Kevlar-reinforced samples.

The variation in flexural modulus across different configurations can be attributed to the complex interplay between fiber alignment, volume fraction, and fiber – matrix interaction. In blank concrete, the material may behave as a relatively homogeneous composite, where stiffness is primarily governed by the bulk matrix (Revilla-Cuesta et al., 2022). When fibers are introduced, they may either enhance or reduce the flexural modulus depending on their ability to carry load within the elastic range (Bentur and Mindess, 1990; Li, 2003). In the case of the 3D rebar and 3D hollow woven fabric configurations, a reduction in flexural modulus, from approximately 1200 MPa to 700 MPa, was observed. This may be attributed to suboptimal stress transfer or fiber misalignment relative to the bending direction, which limits their contribution to initial stiffness (Naaman, 2003). Conversely, the solid 3D woven fabric configuration exhibited a notable increase in flexural modulus, despite its higher fiber content. This result suggests that, in this case, the fibers are more favorably aligned and better bonded to the matrix, enabling them to contribute more effectively to the elastic response. The tightly interlocked structure of the solid configuration likely facilitates improved load sharing between fibers and matrix, thereby enhancing stiffness in addition to tensile strength (Hearle and Chen, 2009). Therefore, we highlight that fiber reinforcement does not universally reduce stiffness; rather, its effect depends strongly on architectural factors such as orientation, distribution, and interface quality (Behera and Dash, 2015).

A comparative analysis of the Kevlar-reinforced concrete configurations shows that mechanical performance varies depending on the type of reinforcement. The compressive strength results indicate that blank concrete performed better than the woven fabric – rein-

Table 4. Flexural Modulus of the Kevlar Reinforced Concrete

No	Configurations	FM (MPa)
1	Blank concrete	1526
2	3D rebar	1200
3	3D hollow woven fabric	700
4	Solid 3D woven fabric	1391

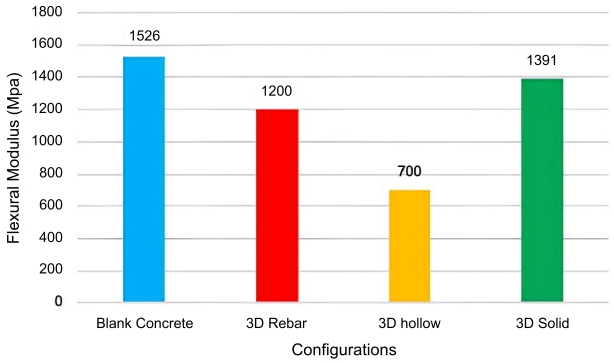

Figure 11 Graphical image of the flexural modulus of the Kevlar reinforcement concrete

forced samples, which may be influenced by the quality of interfacial bonding or microstructural heterogeneity introduced during fiber integration. This observation aligns with the understanding that Kevlar fibers primarily contribute to tensile and post-cracking behavior, rather than enhancing compressive strength. In contrast, the 3D rebar configuration demonstrated higher compressive performance than the woven variants, likely due to improved load transfer at the fiber – matrix interface. While these initial findings are valuable, they are limited to laboratory-scale results obtained under controlled conditions. Therefore, further studies are required to investigate the microstructure, durability under environmental exposure, and scale-dependent performance before recommending specific configurations for structural applications.

However, in flexural testing, Kevlar-reinforced configurations, particularly the 3D solid woven fabric, demonstrated enhanced load-bearing capacity and ductility. These results support earlier observations in the literature regarding Kevlar's effectiveness in improving flexural performance (Williams Portal et al., 2016). Nonetheless, broader claims about cost-effectiveness, long-term material degradation (e.g., in alkaline environments), or practical implementation require further comprehensive studies and are not made at this stage.

4 CONCLUSION

This study investigated the mechanical performance of concrete reinforced with Kevlar fibers configured in various 3-dimensional arrangements, including rebar, hollow woven fabric, and solid woven fabric. The results demonstrate that Kevlar reinforcement significantly influences both the flexural and compressive behavior of the composite material. In compression, the 3D rebar configuration showed the highest strength and stiffness among the reinforced specimens, while woven fabric configurations exhibited relatively lower compressive performance. These outcomes suggest that Kevlar's contribution to compressive properties is limited and potentially influenced by interfacial bonding, porosity, and fiber misalignment. In contrast, flexural tests revealed a marked improvement in bending resistance and ductility, especially for the solid 3D woven fabric configuration, which recorded the highest flexural strength and modulus. The trend of increasing flexural strength with higher fiber content reflects the crack-bridging and energy-dissipating capabilities of Kevlar, particularly under tensile stress.

It is important to note that these findings are based on a limited number of specimens under controlled laboratory conditions. While the observed trends are consistent with previous literature, they should not be generalized to real-world applications without further validation. Future research should include a broader statistical sample, long-term durability testing, microstructural analysis, and evaluation under variable environmental conditions to fully assess the practical viability of Kevlar-reinforced concrete in structural applications. Overall, the results provide valuable insight into the mechanical effects of 3D Kevlar reinforcement in cementitious composites and offer a foundation for future development of high-performance fiber-reinforced concrete systems.

DISCLAIMER

The authors declare no conflict of interest.

ACKNOWLEDGMENTS

We would like to express our sincere gratitude to all those who have contributed to this research. First, we thank Mr. Hardianto, whose guidance and insightful comments throughout the study were invaluable in shaping the direction of this work. We also appreciate the expert analysis and data collection provided by Mrs. Ria wanti, whose assistance in conducting the experiments was essential to the success of this project.

Special thanks go to Dr. Ikbal for their support in the literature review and theoretical framework development, which laid the foundation for this research.

Finally, we would like to acknowledge the funding support from Politeknik STTT Bandung, Ministry of Industry of the Republic of Indonesia under Grant No. 84, 2023, which made this research possible

REFERENCES

Abidin, N. M., Sultan, M. T., Hua, L. S., Basri, A. A., Shah, A. U. M. and Safri, S. N. (2019), 'A brief review of computational analysis and experimental models of composite materials for aerospace applications', *Journal of Reinforced Plastics and Composites* **38**(23-24), 1031–1039.
URL: *https://doi.org/10.1177/0731684419862869*

Aravind, D., Senthilkumar, K., Rajini, N., Kumar, T. S. M., Chandrasekar, M., Ismail, S. O., Yeetsorn, R., Parameswaranpillai, J., Siengchin, S. and Devi, M. I. (2022), 'Feasibility of elastomeric composites as alternative materials for marine applications: A compendious review on their properties and opportunities', *Proceedings of the Institution of Mechanical Engineers, Part M: Journal of Engineering for the Maritime Environment* **236**(4), 839–855.
URL: *https://doi.org/10.1177/14750902221095321*

Bartulović, B., Juradin, S., Žižić, D. and Galić, M. (2022), 'Influence of Cotton Knitted Fabric Waste Addition on

Concrete Properties', *Buildings* **12**(8), 1121.
URL: *https://doi.org/10.3390/buildings12081121*

Behera, B. and Dash, B. (2015), 'Mechanical behavior of 3D woven composites', *Materials & Design* **67**, 261–271.
URL: *https://doi.org/10.1016/j.matdes.2014.11.020*

Bentur, A. and Mindess, S. (1990), *Fibre Reinforced Cementitious Composites (Routledge, Ed.)* , 2 edn, CRC Press. Edited by Routledge.
URL: *https://doi.org/10.1201/9781482267747*

Brameshuber, W. (2006), *Textile Reinforced Concrete*, Vol. 36 of *RILEM Report*, RILEM Publications SARL. State-of-the-Art Report of RILEM Technical Committee TC 201-TRC.

Carneiro da Silva, L. R., de Oliveira Rios, A. and Santana, R. M. C. (2023), 'Polymer blends of poly(lactic acid) and starch for the production of films applied in food packaging: A brief review', *Polymers from Renewable Resources* **14**(2), 108–153.
URL: *https://doi.org/10.1177/20412479231154924*

Cheung, T. W. and Li, L. (2019), 'A review of hollow fibers in application-based learning: from textiles to medical', *Textile Research Journal* **89**(3), 237–253.
URL: *https://doi.org/10.1177/0040517517741164*

Coskun, H. and Oner, E. (2022), 'Development of upholstery electro-fabric for smart textile applications', *Journal of Industrial Textiles* **52**(2_suppl), 2306S–3329S.
URL: *https://doi.org/10.1177/15280837211048157*

Dalkılıç, H., Özdemir, H. and Özcanhan, M. H. (2024), 'Wireless transmission of vital body data and ambient magnetic field with wearable IoT device attached smart textile', *Textile Research Journal* **95**(1-2), 17–26.
URL: *https://doi.org/10.1177/00405175241252964*

El-Feky, M. S., Badawy, A. H., Seddik, K. M. and Yahia, S. (2024), 'Evaluation of polyester high-tenacity fabric and carbon nanotube reinforcements for improving flexural response in concrete beams', *Scientific Reports* **14**(1), 26907.
URL: *https://doi.org/10.1038/s41598-024-76729-8*

Friese, D., Scheurer, M., Hahn, L., Gries, T. and Cherif, C. (2022), 'Textile reinforcement structures for concrete construction applications –– a review', *Journal of Composite Materials* **56**(26), 4041–4064.
URL: *https://doi.org/10.1177/00219983221127181*

Ghasemi, R., Safarabadi, M., Haghighi-Yazdi, M. and Mirdehghan, S. A. (2024), 'Micromechanical modeling and experimental study of the flexural properties of impregnated woven textile-reinforced concrete', *Proceedings of the Institution of Mechanical Engineers, Part L: Journal of Materials: Design and Applications* **238**(9), 1791–1804.
URL: *https://doi.org/10.1177/14644207241233719*

Gopinath, S., Murthy, A. R., Iyer, N. R. and Prabha, M. (2015), 'Behaviour of reinforced concrete beams strengthened with basalt textile reinforced concrete', *Journal of Industrial Textiles* **44**(6), 924–933.
URL: *https://doi.org/10.1177/1528083714521068*

Hahn, L., Hong, S., Treppe, K., von Zuben, M., Rittner, S., Beckmann, M. and Cherif, C. (2021), 'Approach toward a thermodynamic analysis on the drying and curing process of textile reinforcements for construction applications as a basis for continuous process control and optimization', *Journal of Industrial Textiles* **50**(10), 1572–1593.
URL: *https://doi.org/10.1177/1528083719865037*

Hearle, J. W. S. and Chen, X. (2009), 3d woven preforms and properties for textile composites, *in* 'Proceedings of the ICCM International Conferences on Composite Materials'.

Hu, Y., He, Z. and Xuan, H. (2020), 'Impact Resistance Study of Three-Dimensional Orthogonal Carbon Fibers/BMI Resin Woven Composites', *Materials* **13**(19), 4376.
URL: *https://doi.org/10.3390/ma13194376*

Islam, M. J., Ahmed, T., Imam, S. M. F. B., Ifaz, M. and Islam, H. (2023), 'Flexural and impact behavior of textile reinforced concrete panel', *International Journal of Protective Structures* **14**(2), 221–241.
URL: *https://doi.org/10.1177/20414196221095250*

Koeckritz, U., Cherif, C., Weiland, S. and Curbach, M. (2010), 'In-Situ Polymer Coating of Open Grid Warp Knitted Fabrics for Textile Reinforced Concrete Application', *Journal of Industrial Textiles* **40**(2), 157–169.
URL: *https://doi.org/10.1177/1528083709102938*

Krimi, I., Ducoulombier, L., Dakhli, Z. and Lafhaj, Z. (2016), 'Durability of textile facing materials for construction: Operating accelerated ageing protocol results in basic medium for lifetime estimation in conditions of use', *Journal of Industrial Textiles* **46**(3), 929–949.
URL: *https://doi.org/10.1177/1528083715606106*

Laiblová, L., Pešta, J., Kumar, A., Hájek, P., Fiala, C., Vlach, T. and Kočí, V. (2019), 'Environmental Impact of Textile Reinforced Concrete Facades Compared to Conventional Solutions—LCA Case Study', *Materials* **12**(19), 3194.
URL: *https://doi.org/10.3390/ma12193194*

Li, Q. and Xu, S. (2011), 'Experimental Research on Mechanical Performance of Hybrid Fiber Reinforced Cementitious Composites with Polyvinyl Alcohol Short Fiber and Carbon Textile', *Journal of Composite Materials* **45**(1), 5–28.
URL: *https://doi.org/10.1177/0021998310371529*

Li, V. (2003), 'On Engineered Cementitious Composites (ECC) A Review of the Material and Its Applications', *Journal of Advanced Concrete Technology* **1**(3), 215–230.

Lin, T. A., Lin, M.-C., Lin, T. R., Sim, K. S., Lin, J.-H. and Lou, C.-W. (2022), 'High-strength protective polyester textiles incorporated with metallic materials: Characterizations and radiation-shielding effectiveness', *Journal of Industrial Textiles* **51**(10), 1585–1600.
URL: *https://doi.org/10.1177/1528083720904678*

Lyu, L., Wen, F., Lyu, T., Zhou, X. and Gao, Y. (2022), 'Interfacial Modification and Bending Performance of 3D Orthogonal Woven Composites with Basalt Filament Yarns', *Materials* **16**(11), 4015.
URL: *https://doi.org/10.3390/ma16114015*

Mahadik, Y. and Hallett, S. (2022), 'Effect of fabric compaction and yarn waviness on 3D woven composite compressive properties', *Composites Part A: Applied Science and Manufacturing* **42**(11), 1592–1600.
URL: *https://doi.org/10.1016/j.compositesa.2011.07.006*

Naaman, A. E. (2003), 'Engineered Steel Fibers with Optimal Properties for Reinforcement of Cement Composites', *Journal of Advanced Concrete Technology* **1**(3), 241–252.
URL: *https://doi.org/10.3151/jact.1.241*

Najafi, B., Mohseni, H., Grewal, G. S., Talal, T. K., Menzies, R. A. and Armstrong, D. G. (2017), 'An Optical-Fiber-Based Smart Textile (Smart Socks) to Manage Biomechanical Risk Factors Associated With Diabetic Foot Amputation', *Journal of Diabetes Science and Technology* **11**(4), 668–677.
URL: *https://doi.org/10.1177/1932296817709022*

Nelson, P. K., Li, V. C. and Kamada, T. (2002), 'Fracture Toughness of Microfiber Reinforced Cement Composites', *Journal of Materials in Civil Engineering* **14**(5), 384–391.
URL: *https://doi.org/10.1061/(ASCE)0899-1561(2002)14:5(384)*

Neves, R. and Felicíssimo, D. (2020), 'Control of Cracking in Textile Reinforced Concrete with Unresin Carbon Fibers', *Materials* **13**(14), 3209.
URL: *https://doi.org/10.3390/ma13143209*

Nguyen, H., Mutsuyoshi, H. and Zatar, W. (2013), 'Flexural Behavior of Hybrid Composite Beams', *Transportation Research Record* **2332**(1), 53–63.
URL: *https://doi.org/10.3141/2332-06*

Perera, Y. S., Muwanwella, R. M. H. W., Fernando, P. R., Fernando, S. K. and Jayawardana, T. S. S. (2021), 'Evolution of 3D weaving and 3D woven fabric structures', *Fashion and Textiles* **8**(11).
URL: *https://doi.org/10.1186/s40691-020-00240-7*

Revilla-Cuesta, V., Skaf, M., Santamaría, A., Romera, J. M. and Ortega-López, V. (2022), 'Elastic stiffness estimation of aggregate – ITZ system of concrete through matrix porosity and volumetric considerations: explanation and exemplification', *Archives of Civil and Mechanical Engineering* **22**(2), 59.
URL: *https://doi.org/10.1007/s43452-022-00382-z*

Sankaran, V., Ruder, T., Rittner, S., Hufnagl, E. and Cherif, C. (2016), 'A multiaxial warp knitting based yarn path manipulation technology for the production of bionic-inspired multifunctional textile reinforcements in lightweight composites', *Journal of Industrial Textiles* **45**(6), 1188–1203.
URL: *https://doi.org/10.1177/1528083714555778*

Sarwar, A., Bougherara, H. and Zdero, R. (2022), 'Tensile and compressive damage assessment of a novel sandwich composite structure made of Kevlar/flax/epoxy hybrid laminates', *Proceedings of the Institution of Mechanical Engineers, Part L: Journal of Materials: Design and Applications* **236**(9), 1842–1853.
URL: *https://doi.org/10.1177/14644207221085686*

Seyam, A. M., Vallabh, R. and Hassanin, A. H. (2015), 'Improving UV Resistance of Fibers: Idealized Computational Model Predicting the Distribution of UV Blocking Cylindrical Nanoparticles in Protective Polymeric Layer', *Journal of Engineered Fibers and Fabrics* **10**(1).
URL: *https://doi.org/10.1177/155892501501000103*

Shafei, B., Kazemian, M., Dopko, M. and Najimi, M. (2021), 'State-of-the-Art Review of Capabilities and Limitations of Polymer and Glass Fibers Used for Fiber-Reinforced Concrete', *Materials* **14**(2), 409.
URL: *https://doi.org/10.3390/ma14020409*

Ursache, Ș., Cerbu, C. and Hadăr, A. (2024), 'Characteristics of Carbon and Kevlar Fibres, Their Composites and Structural Applications in Civil Engineering-A Review', *Polymers* **16**(1), 127.
URL: *https://doi.org/10.3390/polym16010127*

Verma, V. and Majumdar, A. (2024), 'Structure-property relationships of 3D woven fabric composites: A critical review through bibliometric and content analyses', *Journal of Composite Materials* **59**(2), 241–263.
URL: *https://doi.org/10.1177/00219983241302171*

Walton, P. L. and Majumdar, A. J. (1978), 'Properties of cement composites reinforced with Kevlar fibres', *Journal of Materials Science* **13**(5), 1075 – 1083.
URL: *https://doi.org/10.1007/BF00544703*

Wang, D., Che, J., Liu, C. and Liu, H. (2024), 'Design of Mixture Proportion of Engineered Cementitious Composites Based on Desert Sand', *KSCE Journal of Civil Engineering* **28**(7), 2897–2907.
URL: *https://doi.org/10.1007/s12205-024-1875-9*

Williams Portal, N., Nyholm Thrane, L. and Lundgren, K. (2016), 'Flexural behaviour of textile reinforced concrete composites: experimental and numerical evaluation', *Materials and Structures* **50**(4).
URL: *https://doi.org/10.1617/s11527-016-0882-9*

Wu, C., Pan, Y. and Yan, L. (2023), 'Mechanical Properties and Durability of Textile Reinforced Concrete (TRC)—A Review', *Polymers* **15**(18), 3826.
URL: *https://doi.org/10.3390/polym15183826*

Yan, L. and Chouw, N. (2013), 'A comparative study of steel reinforced concrete and flax fibre reinforced polymer tube confined coconut fibre reinforced concrete beams', *Journal of Reinforced Plastics and Composites* **32**(16), 1155–1164.
URL: *https://doi.org/10.1177/0731684413487092*

Zhang, A., Zhang, D., Li, D., Zhu, H., Xiao, H. and Jia, J. (2010), 'Effects of void content on mechanical properties of carbon/epoxy composite laminates', *Zhongguo Jixie Gongcheng [China Mechanical Engineering]* **21**, 3014–3018.